Liquid Crystals
Publication details, including instructions for authors and subscription information:
http://www.informaworld.com/smpp/title~content=t713926090

Synthesis and frustrated phases of chiral liquid crystals derived from (*R*)-3-alkoxy-2-methylpropionic acids

S. -L. Wu[a]; T. -S. Chen[a]
[a] Department of Chemical Engineering, Tatung University, Taipei, Taiwan 104, ROC

To cite this Article Wu, S. -L. and Chen, T. -S.(2005) 'Synthesis and frustrated phases of chiral liquid crystals derived from (*R*)-3-alkoxy-2-methylpropionic acids', Liquid Crystals, 32: 1, 63 — 68
To link to this Article: DOI: 10.1080/02678290512331324002
URL: http://dx.doi.org/10.1080/02678290512331324002

Liquid Crystals, Vol. 32, No. 1, January 2005, 63–68

Synthesis and frustrated phases of chiral liquid crystals derived from (*R*)-3-alkoxy-2-methylpropionic acids

S.-L. WU* and T.-S. CHEN

Department of Chemical Engineering, Tatung University, 40 Chungshan N. Rd., 3rd Sec., Taipei, Taiwan 104, ROC

(*Received 26 November 2002; in final form 18 September 2004; accepted 29 September 2004*)

A homologous series of chiral compounds, (*R*)-6-(3-alkoxy-2-methylpropionyloxy)-2-naphthyl 4-alkoxybenzoates, *n*MPN*m*B (n=2–5, m=6–13), derived from methyl (*R*)-3-hydroxy-2-methylpropionate, was prepared for the study of mesormorphic phases. The mesophases were determined mainly by their microscopic textures and identified by the racemic modification. The results show that most of these compounds displayed frustrated phases BP, TGB_A^* and TGB_C^*, and the N*phase. Moreover, the thermal stability of the frustrated phases is significantly affected by the length of the alkyl chain in both achiral and chiral groups of the compounds. The spontaneous polarization in the TGB_C^* phase of compounds *n*MPN10B in a surface-stabilized geometry was measured, giving $\mathbf{P}_\text{s}$ values of about 20 nC cm^{-2}.

1. Introduction

The blue phases (BPs) [1–4] and twisted grain boundary (TGB) phases [5–10] are two kinds of frustrated phases that have been of great interest in the field of chiral liquid crystal systems. Many compounds have been synthesized and investigated to account for the appearance of theses phases, and a general structure–property relationship has been established [11]. The results indicated that, to generate these phases, the molecules require optical purity and high chirality that has high twisting power to form a helix. Thus, the optically pure chiral moieties used as building blocks for the preparation of chiral liquid crystals were generally commercially available compounds or synthesized by using chiral auxiliaries.

We have previously developed optically pure (*R*)-3-alkylmercapto-2-methylpropionic acids by using an optically active (D)-2,10-camphorsulpham as a chiral auxiliary [12–14]. Chiral liquid crystals derived from these chiral acids have displayed very rich mesomorphic properties. The results in chiral compounds (*R*)-6-(3-alkylmercapto-2-methylpropionyloxy)-2-naphyl 4-alkyloxybenzoates, *n*MMPN*m*B(n=2–5, m=6–12), showed that these compounds mostly possess the frustrated phases BP, TGB_A^* and TGB_C^*, and the N* phase was found in a rather narrow temperature range [13, 14]. Therefore the structurally similar homologous series of chiral liquid crystals (*R*)-6-(alkoxy-2-methylpropionyloxy)-2-naphthyl 4-alkoxybenzoates, *n*MPN*m*B(n=2–5, m=6–13), derived from commercially available methyl (*R*)-3-hydroxy-2-methylpropionate, was prepared for this study, and the resulting mesophases of these compounds were compared with those of compounds *n*MMPN*m*B. The general structural formulas for compounds *n*MMPN*m*B and *n*MPN*m*B are depicted bellow.

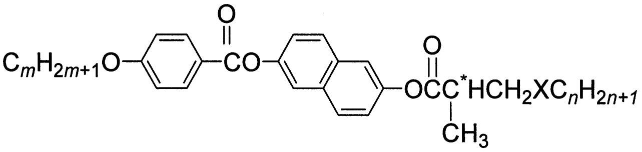

X=S ; *n*MMPN*m*B (n=2–5, m=6–12)
X=0 ; *n*MPN*m*B (n=2–5, m=6–13)

2. Experimental

2.1. *Characterization*

All intermediates and final compounds were isolated by column chromatography and purified by recrystalization. The purity of the products was checked by thin layer chromatography and further confirmed by elemental analysis using a Perkin-Elmer 2400 spectrometer. The chemical structures of compounds were analysed by proton magnetic resonance spectroscopy using a Jeol EX-400 FTNMR spectrometer. The magnitudes of specific rotation [α] for the chiral compounds were measured in anhydrous

---

*Corresponding author. Email: slwu@ttu.edu.tw

Liquid Crystals
ISSN 0267-8292 print/ISSN 1366-5855 online © 2005 Taylor & Francis Ltd
http://www.tandf.co.uk/journals
DOI: 10.1080/02678290512331324002

$CHCl_3$ using a Jasco DIP-360 digital polarimeter. Transition temperatures were determined by a DuPont DSC910 calorimeter at a scanning rate of 1°C min^{-1}. Mesophases of the compounds were identified by the observing textures with a Nikon Microphot-FXA optical microscope under crossed polarizers with a Mettler FP82-HT in connection with an FP80 hot stage as a temperature controller. Homogeneously aligned cells with a thickness of 2 μm were purchased from E. H. C. Co., Japan. The spontaneous polarization ($\mathbf{P}_s$) was measured by the triangular wave method [15].

2.2. *Preparation of the compounds*

Compounds *n*MPN*m*B were prepared by the synthetic procedures outlined in the scheme. The primary hydroxy group of methyl (*R*)-3-hydroxy-2-methylpropionate was alkylated with *n*-alkyl iodide in the presence of silver(I) oxide to give compound **2**(*n*).The ester group of chiral compound **2**(*n*) was hydrolyzed in the presence of potassium hydroxide in aqueous ethanolic solution and then acidified to afford the chiral acids **3**(*n*). Williamson synthesis of 4-hydroxybenzoic acid with alkyl bromide gave alkoxybenzoic acid **5**(*m*). This acid was converted to acid chloride **6**(*m*) by reacting with oxalyl chloride. This was followed by the reaction of acid chloride **6**(*m*) with excess of 2,6-dihydroxynaphthalene in the presence of pyridine to obtain alcohol **7**(*m*). Esterification of the alcohol **7**(*m*) with chiral acids **3**(*n*) by treatment with *N*,*N*′-dicyclohexylcarbodiimide (DCC) and 4-dimethylaminopyridine (DMAP) gave the target compounds. The detailed synthetic procedures are described below.

2.2.1. Methyl (*R*)-3-alkoxy-2-methylpropionates, 2(*n*; *n*=2–5). To a mixture of methyl (*R*)-3-hydroxy-2-methylpropionate (84.71 mmol) and *n*-alkyl iodide (168.8 mmol) was added silver(I) oxide (42.75 mmol) in several portions at 25–30°C. After stirring at the same temperature for 24 h, the reaction mixture was diluted with ether and the silver(I) oxide removed by filtration. The filtrate was evaporated under vacuum to leave an oily residue, which was further purified by distillation under reduced pressure to afford methyl (*R*)-3-alkoxy-2-methylpropionates as viscous oil in 40% yields. Typical example of analytical results for **2**(*n*=2) is given as follows: b.p. 82°C, 40 mm Hg^{-1}; $[\alpha]^{22}_{D}=-13.85$ (c=1.079, $CHCl_3$). ^1H NMR, δ (ppm, CDCl3): 1.05–1.5 (m, 6H), 2.58–2.71 (m, 1H), 3.31–3.42 (m, 2H), 3.51–3.58 (q, 2H), 3.58–3.62 (s, 3H).

2.2.2. (*R*)-3-alkoxy-2-methylpropionic acids, 3(*n*). To a stirred solution of compounds **2**(*n*) (19.2 mmol) in ethanol (16.7 ml) was added dropwise 5M KOH (19.23 mmol) aqueous solution, and the mixture further stirred for 2 h at 3°C. The reaction mixture was poured into 10% HCl and extracted twice with ether. The combined organic layer was washed several times with water and dried over anhydrous magnesium sulphate; it was then concentrated under vacuum and distilled to afford compounds **3**(*n*) as viscous oils. A typical example of analytical results for **3**(*n*=2) is as follows: $[\alpha]^{22}_{D}=-17.03$ (c=1.079, $CHCl_3$). ^1H NMR, δ (ppm, $CDCl_3$): 0.80–1.20 (m, 6H), 2.58–2.71 (m, 1H), 2.26–2.70 (m, 1H), 3.30–3.52 (m, 2H), 3.50–3.58 (q, 2H), 10.3–10.6 (s, 1H).

2.2.3. 4-Alkoxybenzoic acids, 5(*m*; *m*=6–13). A solution of potassium hydroxide (2.8 g, 50 mmol) and potassium iodide (0.6 g, 3.3 mmol) in distilled water (50 ml) was added to a slurry of 4-hydoxybenzoic acid (25 mmol) in ethanol (200 ml), and the mixture heated under reflux for an hour. Alkyl bromide (75 mmol) was then added dropwise and the mixture heated a further 12 h under reflux. Aqueous potassium hydroxide (100 ml, 10%) was added and reflux continued for 2 h. After cooling, the mixture was acidified by the addition of 5% HCl and filtered. The crude product was washed with cold water and recrystallized from glacial acetic acid and ethanol; a 70% yield of compound **5**(*m*) was obtained.

2.2.4. 4-Alkoxybenoic acid chlorides, 6(*m*). Compounds **5**(*m*) (5 mmol) were reacted with oxalyl chloride (15 mmol) in dichloromethane (6 ml) at reflux temperature for 2 h under nitrogen. After excess oxalyl chloride was completely removed, the precipitates were used for the subsequent reaction.

2.2.5. 6-Hydroxy-2-naphthyl 4-alkoxybenoates, 7(*m*). Compounds **6**(*m*) dissolved in dichloromethane (3 ml) were added dropwise to the mixture of 2,6-dihydroxynaphthalene (15 mmol), dried pyridine (5 ml) and anhydrous tetrahydrofuran (5 ml). The reaction mixture was cooled in a refrigerator for 2 days. Silica gel was then added to the mixture, which was then dried and powdered. The product was collected by column chromatography over silica gel (70–230 mesh) using dichloromethane as eluent. After recrystallization from absolute ethanol, a 75% yield of white precipitate was obtained. The analytical results for an example of **7** (*m*=10) are as follows. Elemental analysis for $C_{27}H_{32}O_4$: calcd, C 76.44, H 7.90; found, C 77.05, H 7.88%. ^1H NMR, δ (ppm, $CDCl_3$): 8.80–1.90 (m, 19H), 4.0–4.1 (t, 2H), 5.2–5.4 (s, 1H), 6.9–8.2 (m, 10H).

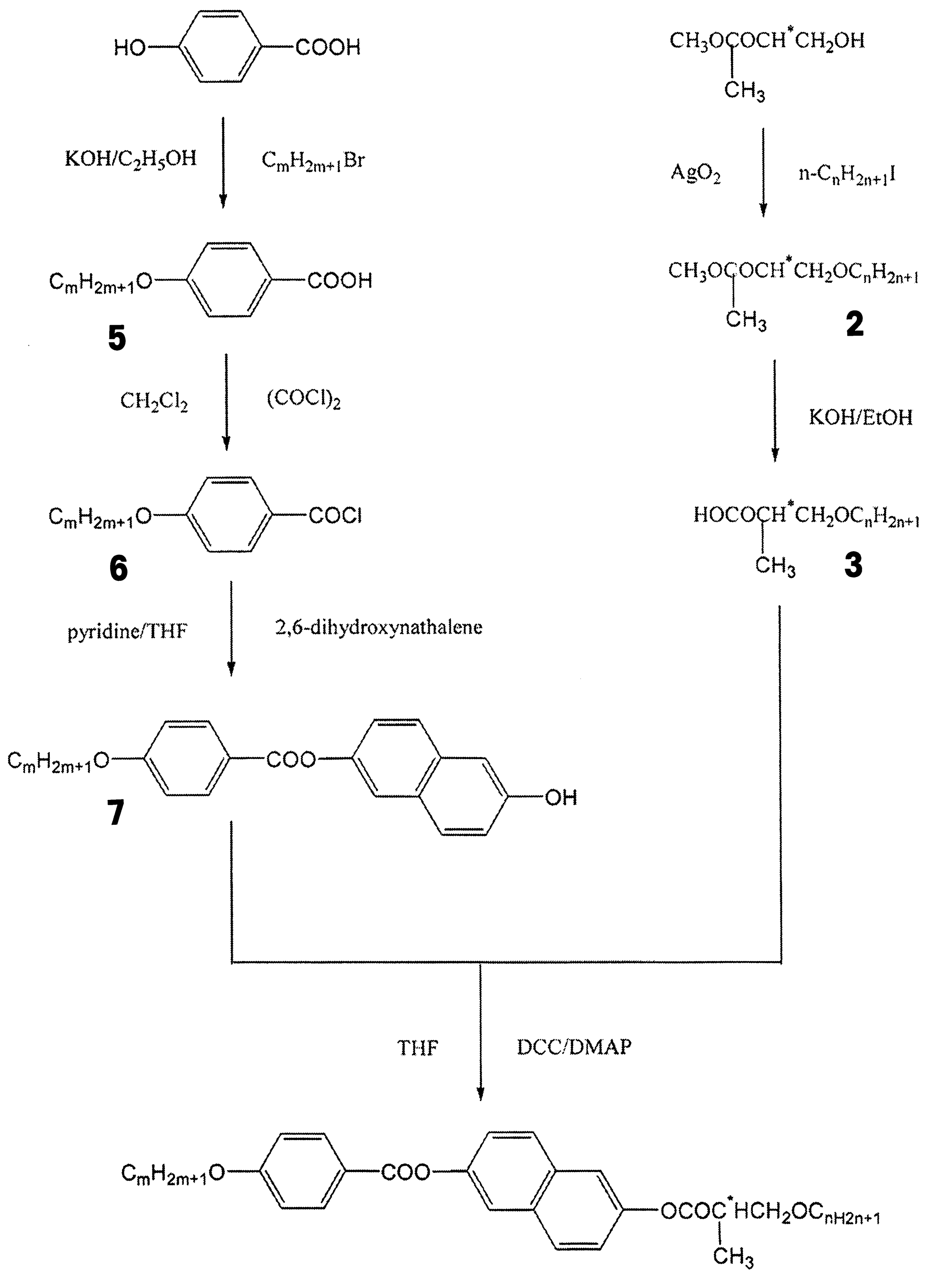

Scheme. Synthetic procedures for the compounds *n*MPN*m*B.

2.2.6. (*R*)-6-(Alkoxy-2-methylpropionyloxy)-2-naphthyl 4-alkoxybenzoates, nMPNmB. A mixture of compound **7**(*m*) (1.48 mmol), compounds **3**(*n*) (1.35 mmol), DCC (1.85 mmol), DMAP (0.148 mmol) and anhydrous tetrhydrofuran (8 ml) was stirred at room temperature for 4 days. After the work-up procedure, the product was isolated by column chromatography over silica gel (70–230 mesh) using dichloromethane as eluent and recrystallized from absolute ethanol; 60–75% yields of white precipitate were obtained. The analytical results for an example of *n*MPN*m*B(*n*=2, *m*=10) are given as follows. Elemental analysis for $C_{33}H_{32}O_6$: calcd, C 76.69, H 7.59; found, C76.62, H 7.59. ^{1}H NMR, δ (ppm, $CDCl_3$): 0.80–1.90 (m, 25H), 2.9–3.1 (m, 1H), 3.5–3.7 (q, 2H), 3.7–3.8 (d, 2H), 3.9–4.1(t, 2H), 6.9–8.3 (m, 14H).

3. Results and discussion

Mesophases were principally identified by the microscopic textures. The blue phase (BP) was characterized by the formation of blue fog texture and the N* phase was demonstrated by the existence of paramorphotic texture. The TGB_A^* phase was identified by the appearance of spiral filament texture [13, 14, 16], and the TGB_C^* phase by the appearance of coloured spiral filament texture accompanied with striated desclination lines [13, 14, 16, 17]. The texture of the racemic mixture for compounds (*R*)-2MPM10B and (*S*)-2MPN10B were investigated, and resulted in the mesophases N, SmA and SmC.

The mesophases and their corresponding phase transition temperatures measured by DSC for compounds 2MPN*m*B are listed in table 1; the phase diagram as a function of alkyl chain length *m* is plotted in figure 1. Three stable frustrated phases, BP, TGB_A^* and TGB_C^*, are found in this series of compounds. Compound 2MPN6B exhibits BP and N* phases. Extension of the achiral alkyl chain ($m \geq 7$) favours the formation of TGB_A^* phase, but their stability is suppressed by the appearance of the TGB_C^* phase ($m \geq 8$). When the alkyl chain length is extended to *m*=12, the TGB_A^* phase disappears, accompanied by a N*–TGB_C^* phase transition. It seems that as *m* increases, the stability of the TGB_A^* phase falls and that of the TGB_C^* phase increases, similar to that observed with sulphur-containing homologues [13]. The thermal stability of the frustrated phases indicated that the compounds possess high degree of chirality [11].

The mesophases and their corresponding phase transition temperatures for compounds *n*MPN10B are listed in table 2; the phase diagram as a function of alkyl chain length *n* is plotted in figure 2. It can be seen that the lengthening of alkyl chain *n* suppresses the formation of the TGB_A^* phase but favours the formation of the TGB_C^* phase. Recent studies have shown [14] that trapping or restricting the motion of the chiral centre, by increasing the length of the terminal aliphatic chain appended to the chiral tail, will damp the rotational freedom, resulting in an increased effect on the chirality. The diminishing of rotational freedom by the extension of the chiral tail enables the molecules to pack easily. Thus, as the alkyl chain steadily lengthens from ethyl to pentyl in compounds *n*MPN10B, the thermal stability of the TGB_C^* phase gradually increases. It was found that the thermal stability of the BP phase also increases due to the gradual increase in chirality.

The mesomorphic properties of compounds *n*MPN10B were compared with those of compounds *n*MMPN10B [14]. As the ethyl group at the chiral tail of the oxygen-containing materials extends to pentyl, the TGB_A^* phase is suppressed and a relatively wide

Table 1. Mesophases, transition temperatures (°C) and enthalpies ($J\,g^{-1}$) (in italics) for compounds 2MPN*m*B on cooling. [ ] indicates a monotropic transition.

Compound	I		BP		N*		TGB_A*		TGB_C*		Cr	m.p.
2MPN6BC	•	85.9 [c]	•	82.9[a] *0.6*	•		—		—	50.2 *19.71*	•	77.9 *25.95*
2MPN7BC	•	76.0	•	64.9[a]	•	[51.9][a] *1.16*[b]	•		—	38.6 *28.96*	•	53.6 *35.79*
2MPN8BC	•	80.0 *0.41*	•	73.9[a] [c]	•	64.0[a] *1.06*	•	[50.3][a] [c]	•	48.1 *24.22*	•	63.2 *29.37*
2MPN9BC	•	76.8 *0.7*	•	69.9[a]	•	64.8[a] *0.53*[b]	•	61.0[a] *0.06*	•	34.2 *24.58*	•	58.7 *31.77*
2MPN10BC	•	76.3 *0.69*	•	72.7[a]	•	69.9[a] *0.88*[b]	•	65.9[a] *0.07*	•	36.6 *21.48*	•	48.5 *22.67*
2MPN11BC	•	80.6	•	74.9[a] *0.45*	•	68.0[a] *0.05*	•	67.5[a] [c]	•	37.7 *22.41*	•	52.2 *28.13*
2MPN12BC	•	78.7 *0.74*	•	75.7[a] *0.30*	•	68.0[a] *0.05*	—		•	36.4 *20.74*	•	53.7 *37.61*
2MPN13BC	•	79.8 *0.6*	•	76.7[a] *0.19*	•	74.8[a] *0.03*	—		•	46.2 *29.82*	•	52.1 *29.64*

[a] Determine by thermal optical microscopy.

[b] ΔH(BP–N*–TGB_A).

[c] The enthalpy of the phase transition was too small to determine by DSC.

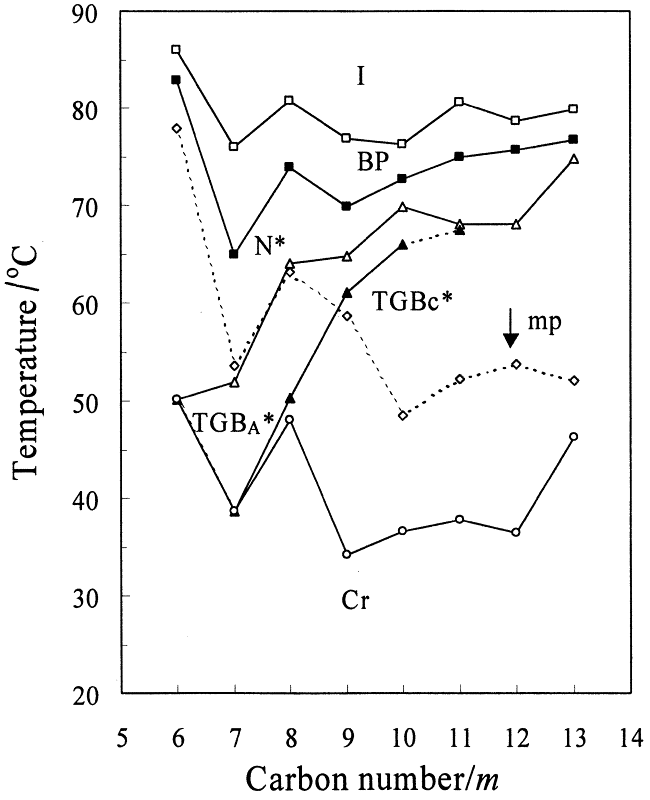

Figure 1. Phase diagram for the transition temperature as a function of alkyl chain length for compounds 2MPN*m*B (*m*=6–13) on cooling. □ I–BP, ■ BP–N*, △ N*–TGB$^*_A$, ▲ TGB$^*_A$–TGB$^*_C$ or N*–TGB$^*_C$, ○, TGB$^*_A$–Cr or TGB$^*_C$–Cr.

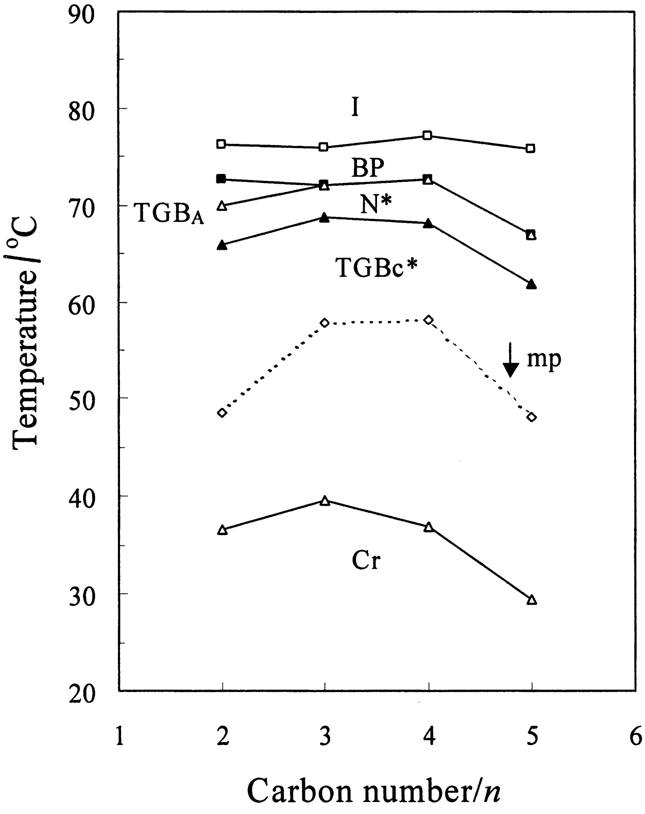

Figure 2. Phase diagram for the transition temperature as a function of alkyl chain length for compounds *n*MPN10B (*n*=2–5) on cooling. □ I–BP, BP–N* or N*–TGB$^*_A$, ▲ TGB$^*_A$–TGB$^*_C$ or N*–TGB$^*_C$, △ TGB$^*_C$–Cr.

temperature range of TGB$^*_C$ phases is obtained; whereas in the sulphur-containing materials, the thermal stability of both TGB$^*_A$ and TGB$^*_C$ phases remains constant. It seems that oxygen, due to its relatively smaller size, allows the molecules to pack more easily than the sulphur-containing materials. It has also been pointed out [18] that when oxygen is replaced by sulphur in the chain, the transverse dipole moment decreases and intermolecular interaction also decreases. Furthermore, the bonding angle C–S–C (99°) is smaller than C–O–C (111°), and the sulphur atom is significantly larger than the oxygen (van der Vaals radii are 1.8 and 1.4Å, respectively). Consequently, the chiral tail in the sulphur-containing materials is more favourable for rotatation about the long axis of the molecule, thereby increasing the free rotation volume of the molecule.

Table 2. Mesophases, transition temperatures (°C) and enthalpies (J g^{-1}) (in italics) for compounds *n*MPN10B on cooling.

Compound	I		BP		N*		TGB$^*_A$		TGB$^*_C$		Cr	m.p.
2MPN10BC	•	76.3	•	72.7[a]	•	69.9[b]	•	65.9[b]	•	36.6	•	48.5
		0.69				*0.88*[c]		*0.07*		*21.48*		*22.67*
3MPN10BC	•	76.0	•	72.0[b]	•		—	68.8[b]	•	39.6	•	57.9
		0.95		*0.2*[b]				*0.04*		*23.62*		*30.86*
4MPN10BC	•	77.1	•	72.7[b]	•		—	68.1[b]	•	36.9	•	58.1
		0.85		*0.07*				*0.02*		*23.3*		*25.86*
5MPN10BC	•	75.8	•	67.1[b]	•		—	61.9[b]	•	29.4	•	48.1
		0.66		*0.07*[a]						*17.07*		*26.67*

[a] Determined by thermal optical microscopy.
[b] Δ*H*(BP–N*).
[c] Δ*H*(BP–N*–TGB$^*_A$).

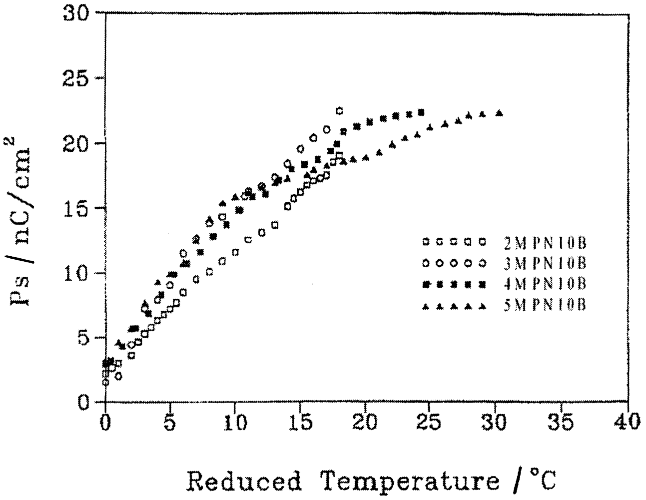

Figure 3. Spontaneous polarization as a function of temperature for compounds *n*MPN10B (*n*=2–5).

This, in principle, increases the steric hinderance between neighbouring molecules, thereby reducing the molecular ordering of the system and consequently suppressing the $\mathrm{TGB}_\mathrm{C}^*$ phase and favouring formation of the $\mathrm{TGB}_\mathrm{A}^*$ phase.

The $\mathbf{P}_\mathrm{s}$ values for compounds *n*MPN10B were measured as a function of temperature in 2 µm homogeneously aligned cells. It has been shown that both $\mathrm{TGB}_\mathrm{A}^*$ and $\mathrm{TGB}_\mathrm{C}^*$ phases in the surface-stabilized geometry may be converted to normal SmA* and SmC* phases by the application of an electric field, resulting in electroclinic and ferroelectric switching, respectively [17]. The $\mathbf{P}_\mathrm{s}$ values for compounds *n*MPN10B, related to the Curie points $T_{\mathrm{SmA^*\text{–}SmC^*}}$ or $T_{\mathrm{N^*\text{–}SmC^*}}$, and recorded at a frequency of 200 Hz and an amplitude of 118.2 $\mathrm{V_{p-p}}$, are shown in figure 3. The saturated polarization values obtained are about 20 nC cm^{-1}, close to that obtained for compounds *n*MMPN10B. The $\mathbf{P}_\mathrm{s}$ values are expected to increase with increasing length of the chiral tail, due to increasingly hindered rotation of the tail; however, the results show that there is no correlation between spontaneous polarization and chiral tail length. This may be because the polarization values are so low that the differences in the values are within the experimental error.

4. Conclusions

The homologous series of chiral compounds, *n*MPN*m*B, has been demonstrated to possess frustrated phases. The thermal stability of these phases is significantly affected by the variation in length of alkyl chain both in achiral and chiral terminal groups of the compounds. Lengthening the alkyl chain in both chiral and achiral groups favours the formation of $\mathrm{TGB}_\mathrm{C}^*$ phase.

References

[1] D. Coates, G.W. Gray. *Phys. Lett.*, **45A**, 115 (1973).
[2] D. Armitage, F.P. Piece. *J. appl. Phys.*, **47**, 2735 (1876).
[3] H. Stegemeyer, T.H. Blumel, K. Hiltrop, H. Onuesseit, F. Porsch. *Liq. Cryst.*, **1**, 3 (1986).
[4] P.P. Crooker. *Liq. Cryst.*, **5**, 751 (1989).
[5] J.W. Goodby, M.A. Waugh, S.M. Stein, E. Chin, R. Pindak, J.S. Patel. *Nature*, **337**, 449 (1989).
[6] J.W. Goodby, M.A. Waugh, S.M. Stein, E. Chin, R. Pindak, J.S. Patel. *J. Am. chem. Soc.*, **111**, 8119 (1989).
[7] H.T. Nguyen, A. Boughta, L. Navailles, P. Barois, N. Isaert, R.J. Twieg, A. Maroufi, C. Destrade. *J. Phys. II(Fr.)*, **2**, 1889 (1992).
[8] R.F. Shao, J.H. Pang, N.A. Clark, J.A. Rego, D.M. Walbl. *Ferroelectrics*, **147**, 255 (1993).
[9] A.J. Sleney, J.W. Goodby. *J. mater. Chem.*, **1**, 5 (1991).
[10] C.J. Booth, D.A. Dummur, J.W. Goodby, J.S. Kang, K.J. Toyne. *J. mater. Chem.*, **4**, 747 (1994).
[11] J.W. Goodby, A.J. Slaney, C.J. Booth, I. Nishyama, J.D. Yuijk, P. Styrng, K.J. Toyne. *Mol. Cryst. liq. Cryst.*, **243**, 231 (1994).
[12] S.L. Wu, F.K. Huang, B.J. Uang, W.J. Tasi. *Liq. Cryst.*, **18**, 715 (1995).
[13] S.L. Wu, J.H. You, B.J. Uang. *Liq. Cryst.*, **28**, 69 (2001).
[14] S.L. Wu, K.J. Wang, M.J. Yu. *Ferroelectrics*, **276**, 93 (2002).
[15] K. Miyasato. *Jpn. J. appl. Phys.*, **22**, 1661 (1983).
[16] S.L. Wu, W.J. Hsieh. *Liq. Cryst.*, **21**, 783 (1996).
[17] R.F. Shao, J.H. Pang, N.A. Clark, J.A. Rego, D.M. Walba. *Ferroeletrics*, **147**, 255 (1993).
[18] W.K. Robision, R.J. Miller, H.F. Gleeson. *Ferroelectrics*, **180**, 291 (1996).